NI ZONED NANO-PYRRHOTITE FROM STARDUST TRACK C2062,2,162 (CECIL)

Z. Gainsforth[1], R. C. Ogliore[2], K. Bustillo[3], A. J. Westphal[1], A. L. Butterworth[1], [1]Space Sciences Laboratory, University of California, Berkeley, CA 94720, USA, [2]Hawai'i Institute of Geophysics and Planetology, University of Hawai'i at Manoa, Honolulu, HI 96822, USA, [3]National Center for Electron Microcopy, Lawrence Berkeley National Laboratory, Berkeley, CA 94720, USA.

Introduction: Bulk Fe-XANES analysis of samples returned from the comet Wild 2 by the Stardust mission estimate that about 1/6 of the iron present is in the form of iron sulfide[1]. Understanding the formation of these sulfides is very important to understanding the distribution of S in the solar system and the history of comet Wild 2. Most of the sulfides found in Wild 2 by TEM are pyrrhotite. Here we discuss the possible origins of a 300 nm diameter pyrrhotite found in Stardust track C2062,2,162.

Experimental: Cecil is a terminal particle of track C2062,2,162 which was embedded in epoxy and ultramicrotomed into slices approximately 80 nm thick at the National Center for Electron Microscopy (NCEM). It was then examined in a Zeiss Libra 200 MC at 200 keV with an omega energy filter and an FEI Titan TEM at 80 keV with a Bruker 4-element EDS detector with a solid angle of 0.7 sr. In the Titan, we acquired two high resolution EDS maps. The first had a probe current of 1 nA for 4 minutes, and the second 1.7 nA for an hour. The compositions from the maps are equivalent within noise. Before and after HAADF images also do not show significant modification of the sulfide. Brightfield imaging and electron diffraction were done before the 1 hour EDS map.

Results: Cecil is a complicated silicate assemblage containing Fe-rich olivine, glass, Na-, Fe-rich pyroxene and sulfides. The sulfides exhibit a range of compositions including Ni-rich (probably pentlandite), and pyrrhotite. In several cases, the Ni-rich sulfide and pyrrhotite are in contact. Most sulfides are submicron in size, with the largest observed sulfide being one micron in length on the long axis.

A 300 nm pyrrhotite was especially remarkable. A bright field image taken along the [110] zone axis is shown in Fig. 1 along with a selected area diffraction pattern. EDS mapping measured an average of 3 wt% Ni, and 120 ppm Se. The Ni was zoned and varied smoothly by a factor of four in concentration over a range of 300 nm (Fig. 2, Fig. 3). The zoning profile is best fit by an exponential with a characteristic length scale of ≈200 nm. The Ni content is close to the chondritic value of Fe/Ni = 17.

While the average composition is $\approx(Fe+Ni)_{0.99}S$, electron diffraction shows the presence of a disordered 6C superlattice structure, indicating that it is pyrrhotite, not troilite. The superstructure is heavily disordered with 6C superlattice spots appearing very diffuse. Additionally, due to zoning, the exact composition is a strong function of position, with (Fe+Ni)/S varying locally by ≈10% (Figure 3).

The grain is surrounded by a 25 nm thick layered silicate and oxide rim. In patches at the surface of the sulfide, there is a slight increase in Ni concentration. Over these patches resides an O-rich layer about 5 nm thick containing Si, Fe, S, Ni, P, Ca, Cl, and K in approximate order of decreasing concentration. Surrounding the entire particle is a uniform rim with similar composition but significantly more Si.

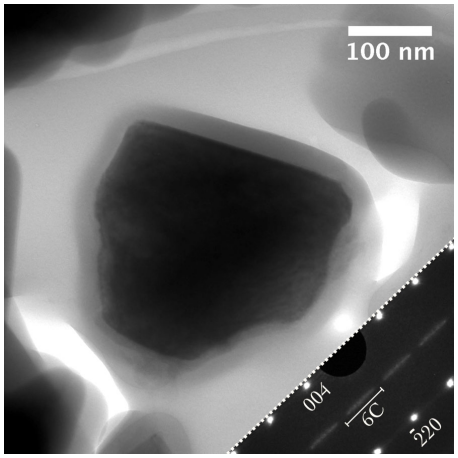

Figure 1: Energy filtered bright field image of the pyrrhotite along the [110] axis. The pyrrhotite is euhedral and approximately 1/2 of a hexagon. Compare Dai and Bradley [11, figure 5]. A 25 nm silicate rim is clearly visible here. Inset lower right is an energy filtered selected area diffraction pattern showing disordered 6C superlattice reflections.

Discussion: Ideal 6C pyrrhotite should have a stoichiometry of $Fe_{11}S_{12}$. However, the diffuse character of our superlattice indicates that it may not be a true 6C superlattice, but rather a disordered lattice consisting of local periodicities up to, but not longer than 6 unit cells. This would be able to accommodate variable cation concentrations such as seen in figure 3. Indeed disordered 6C pyrrhotites are not uncommon in anhydrous IDPs and a strikingly similar grain was found in IDP U222B28 by Dai and Bradley [11, figure 5].

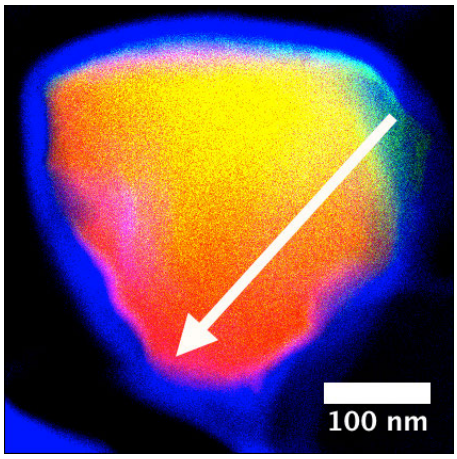

Figure 2: FeNiO RGB map of a pyrrhotite in Cecil showing Ni zoning, and an SiO_2 rich rim approximately 25 nm thick. Ni is heavily concentrated in the upper right (green) and around the bottom periphery of the grain (slight purple rim). The arrow shows the line profile in figure 2.

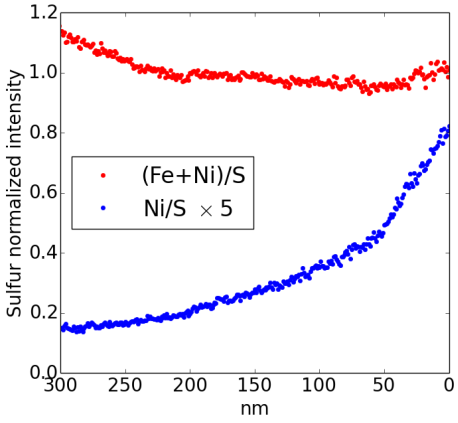

Figure 3: Zoning profile from figure 2 in atomic fractions normalized to S. Ni concentration is approximately exponential from the lower left to the top right in figure 2. (Fe+Ni) shows a slight drop in concentration relative to S.

Lauretta et al [3] experimentally determined the properties of sulfides produced by sulfidation of nebular metal and found that Ni concentration increases with distance from the sulfide/metal interface, and that metal/S decreases with distance from the interface. The zoning profiles shown for the nanosulfide in Cecil (Fig. 3) appear to be consistent with this prediction. In this case, the sulfide/metal surface would be located to the lower left in Fig. 2.

Initial sulfidation is expected to result in troilite, not pyrrhotite. However, Dai and Bradley [11] and other researchers find a preponderance of pyrrhotite, not troilite in IDPs and primitive meteorites which led Zolensky and Thomas [9] to theorize that troilites might be converted directly into pyrrhotite shortly after the Fe metal to troilite conversion. It is not clear, however, what effect this conversion would have had on the zoning in Cecil. If the Ni zoning was preserved in this process, then this grain could be a primary condensate.

As can be seen in Fig. 1, the silicate rim is strikingly uniform and completely surrounds the sulfide which appears dark with a uniform halo, and glassy material surrounding. Each of these phases (sulfide, rim, matrix) is apparently bound to the next. The silicate rim bears a complex chemistry that could reflect its embayment within the larger terminal particle, or it may reflect a history prior to agglomeration. If it were a condensation rim grown on the surface of the sulfide, then the high concentration of elements such as P, Ca and Cl would likely have diffused into it during its residence within the assemblage, or during the process that embedded it in the assemblage. On the other hand, since the silicate rim is amorphous, and the silicate matrix surrounding the silicate rim is also amorphous, it seems problematic to invoke an igneous origin for it.

Given the Ni zoning, and the presence of the silicate rim, we hypothesize that this particle was originally a nebular condensate FeNi metal which reacted with H_2S to produce troilite. Further sulfidation and/or disequilibrium during formation converted it to pyrrhotite. Subsequently, a Si rich rim later condensed onto the surface of the particle, probably before incorporation into Wild 2. This process may be similar to the fine grained material embedded in amorphous silicate recently reported by Stodolna et al. [13] in a Stardust sample.

An alternate interpretation may be that the Ni content was introduced by hydrothermal alteration. The presence of Ni-rich sulfides elsewhere in the terminal particle favors this explanation. However, in an examination of 22 hydrous IDPs, Zolensky and Thomas [9] found no evidence for zoning among similarly sized sulfides.

References:

[1] Westphal, A. J. (2009) *ApJ* 694, 18–28 [2] Ogliore, R. C. et al (2012) 43rd LPSC [3] Lauretta, D. S. et al. (1996) *Icarus*, 122, 288-315[4] Reitmeijer, F. J. M. (2013) *MAPS* 48, 8, 1427-1439 [5] Gainsforth, Z. et al (2013) 44th LPSC [6] Stimac, J. and Hickmott, D. (1994) *Chemical Geology*, 117, 313-330 [7] Fleet, M. E. and Stone, W. E. (1991) *Geochim. et Cosmochim. Acta,* 55, 245-253 [9] Zolensky, M. E. And Thomas, K. L. (1995) *Geochim. et Cosmochim. Acta,* 59, 4707-4712 [10] Luttrell, G.W. (1959) *Geological Survey Bull.* 1019-M [11] Dai, Z. R. and Bradley, J. P. (2001) *Geochim. et Cosmochim. Acta,* 65, 3601-3612 [12] Pósfai, M. et al. (2000) *Am. Min.* 85, 1406-1415 [13] Stodolna, J. et al. (2014) *Earth & Planet. Sci. Lett.*, in press.